2014 IEEE/ASME International Conference on
Advanced Intelligent Mechatronics (AIM)
Besançon, France, July 8-11, 2014

Analytical Study on Increasing Isotropy of Intrinsic Stiffness in Manipulators through Biarticular Structure

Valerio Salvucci[1], Travis Baratcart[1], and Takafumi Koseki[1]

Abstract— **When robots and humans interact in a task, stiffness is necessary for performance, while passive compliance is fundamental for safety. These two factors are the motivation for intrinsic compliant modulation in robots interacting with humans. Variable Stiffness Actuators (VSAs) allow for simultaneous position and stiffness control of a joint, and therefore have been implemented in the realization of intrinsically compliant and high performance manipulators. Most applications employ VSAs in a monoarticular structure, in which one actuator drives one joint. In the biological world however, biarticular muscles (muscles spanning two joints) play a fundamental role in motion control for humans, reducing link inertia and increasing isotropy of end effector force. In this work, a two-link planar manipulator actuated with VSAs in two different actuation structures (the traditional monoarticular and human-like biarticular) is taken into account. The end effector stiffness in both actuation structures is calculated and analyzed. In comparison with the VSA monoarticular structure, the end effector stiffness in the VSA biarticular structure shows a higher isotropy in the region of the workspace favorable for executing dynamic tasks in contact with the environment.**

I. INTRODUCTION

When robots operate in presence of humans passive compliance is fundamental to guarantee safety [1]. A widely known approach to achieve passive compliance is through the use of elastic elements between the actuator and the joint, namely Series Elastic Actuators (SEAs) [2]. A limit of SEAs is that the compliance can not be varied without the use of feedback control as it depends on the mechanical characteristics of the elastic elements, which are constant [3]. In order to overcome the bandwidth limitations of feedback control, while at the same time allowing for passive compliance regulation, Variable Stiffness Actuators (VSAs) are rising in interest. VSAs allow for simultaneous position and stiffness control of a joint by the use of two actuators, therefore they are used in the design of intrinsically compliant manipulators [4], [5], [6], [7], [8].

Unlike traditional robot arms with monoarticular actuation, humans and animals incorporate biarticular muscles — muscles that span two consecutive joints — to regulate stiffness stabilizing unstable dynamics (for example running over rough terrain [9]), to increase accuracy of movement [10], and to transfer power from proximal to distal joints [11].

[1]V. Salvucci, T. Baratcart, and T. Koseki are with Department of Electrical Engineering and Information System, The University of Tokyo, 3–7–1 Hongo, Bunkyoku, Tokyo, 113–8656, Japan valerio at koseki.t.u-tokyo.ac.jp, t_bartcart at koseki.t.u-tokyo.ac.jp, takafumikoseki at ieee.org

Moreover, biarticular muscles appear primarily responsible for the control of the external force direction on the ground [12]. For these reasons interest in robots with biarticular actuators has been rising.

In mechatronic applications, biarticular actuators have been proposed in order to overcome many limitation of conventional actuation structure. It has been shown that, biarticular actuators dramatically increase the range of end effector impedance which can be achieved without feedback [13], increase the capability of path tracking and disturbance rejection, [14] allow for precise output force control [15], and improve balance control for legged robots without force sensors [16]. In addition, biarticularly actuated manipulators produce a maximum output force at the end effector in a more homogeneously distributed way [17].

Regarding hardware design, biarticularly actuated robots have been realized by means of linear actuators [18], [19], and motors with transmissions systems based on pulleys [20], planetary gears [21], wires [22], [23], and passive springs [24]. In [25] a robot finger with VSAs and biarticular actuation structure is proposed, but the influence of the biarticular actuation structure on the end effector isotropy is not investigated.

Stiffness isotropy at the end effector is a fundamental aspect taken into account in the design of robot manipulators. A high isotropy of the stiffness at the end effector is desirable in order to better cope with the nonlinearities resulting from the robot arm geometry (i.e. Jacobian matrix).

In this work, the influence of biarticular actuation structure on the stiffness isotropy resulting at the end effector is analyzed. A two-link planar robot arm with VSAs and two different actuation structures — the traditional monoarticular and human-like biarticular — is taken into account. The end effector compliance in both actuation structures is calculated, and a comparison is carried out.

The paper is organized as follows. Modeling of biarticularly actuated robot arms is shown in section II. In section III the variable stiffness mono- and bi-articular actuator structures are illustrated together with their mathematical modeling. In section IV the analysis method used to compare the two actuation structures is described. The results are shown and analyzed in section V. Finally, conclusions are in section VI.

II. MODELING BIARTICULAR ACTUATION IN ROBOT ARMS

In conventional robot arms each joint is driven by one actuator. On the other hand, animal and human limbs present

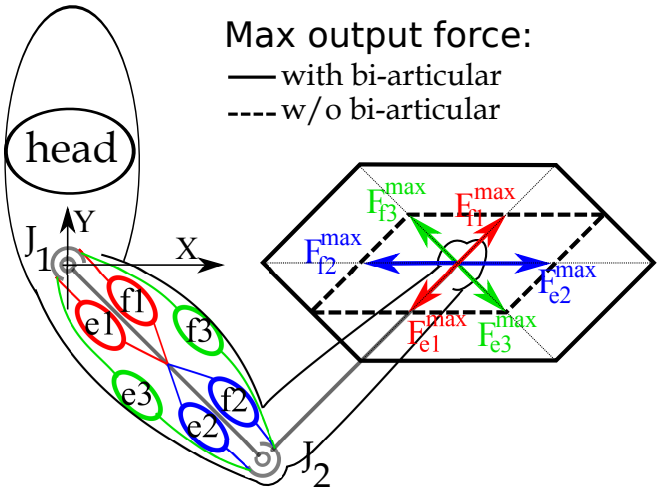

(a) Model and resulting forces at the end effector

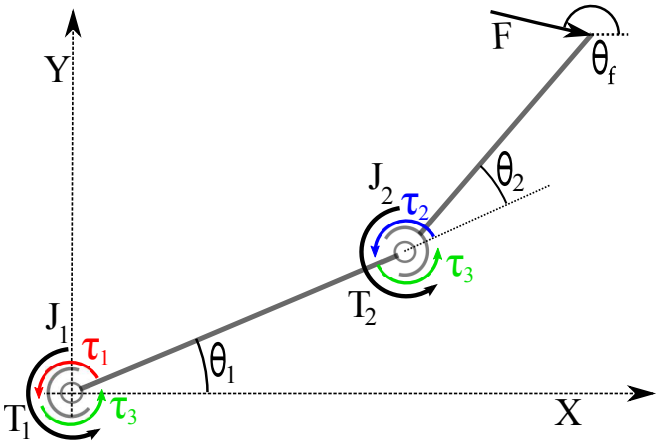

(b) Statics

Fig. 1. Two-link arm with four mono- and two bi-articular actuators

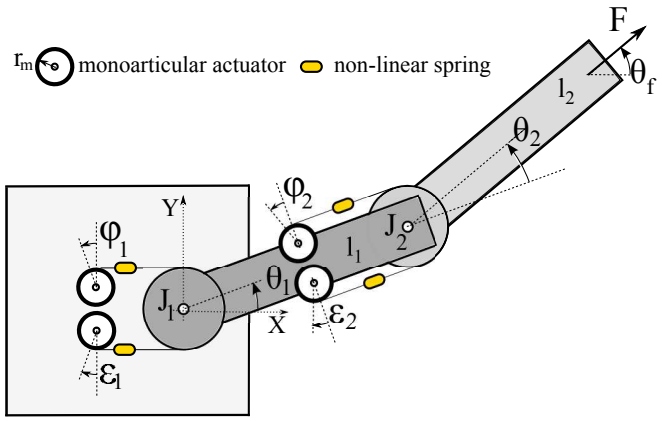

(a) Two monoarticular VSAs (VSMA)

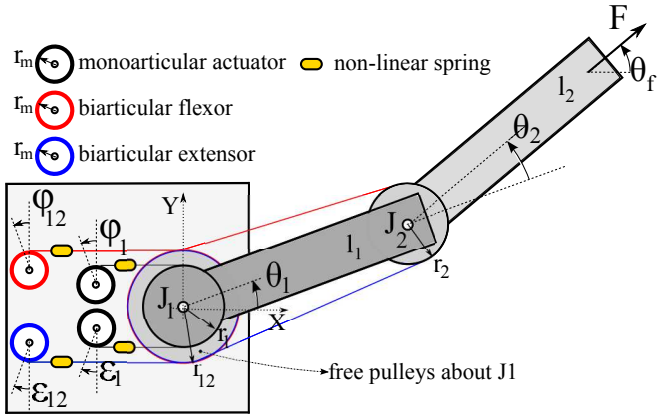

(b) One mono- and one bi-articular VSA (VSBA)

Fig. 2. Two-link intrinsically compliant manipulators: conventional (VSMA) and proposed (VSBA) structures

a complex musculo-skeletal structure based on mono- and multi- articular muscles:

1) Mono-articular muscles produce a torque about one joint.
2) Multi-articular muscles produce torque about more than one joint.

A widely used simplified model of the complex animal musculo-skeletal system [26], [27], [28], [29], is shown in Fig. 1(a).

This model is based on six contractile actuators — three extensors (e1, e2, and e3) and three flexors (f1, f2, and f3) — coupled in three antagonistic pairs:

- e1–f1 and e2–f2: couples of mono-articular actuators producing torques about joint 1 and 2, respectively.
- e3–f3: couple of biarticular actuators producing torque about joint 1 and 2 at the same time.

The six actuators produce contractile forces e_i or f_i for $i=(1,2,3)$ with respective maximum value e_i^m or f_i^m. The resulting end effector forces are $F_{e1}, F_{f1}, F_{e2}, F_{f2}, F_{e12}$, and F_{f12} with respective maximum values $F_{e1}^{max}, F_{f1}^{max}, F_{e2}^{max}, F_{f2}^{max}, F_{e12}^{max}$, and F_{f12}^{max}. The resulting forces at the end effector are shown in Fig. 1(a). If only mono-articular muscles are considered, there are four resulting forces at the end effector and the maximum output force space is a quadrilateral. On the other hand, if biarticular actuators are added, there are six forces at the end effector, hence the maximum output force space becomes an hexagon. The resulting statics are shown in Fig. 1(b) where $\boldsymbol{F}$ is a general force at the end effector; $\boldsymbol{T}=[T_1,T_2]^T$ are total torques about joints 1 and 2, respectively; $\boldsymbol{\tau}$ represents the actuators torques: τ_1 and τ_2 are torques produced by mono-articular actuators about joints 1 and 2, respectively, while τ_3 is the biarticular torque produced about both joints simultaneously. The resulting joint torques are:

$$\boldsymbol{T}=\boldsymbol{B}\boldsymbol{\tau}=\begin{bmatrix}1&0&1\\0&1&1\end{bmatrix}\begin{bmatrix}\tau_1\\\tau_2\\\tau_3\end{bmatrix} \quad (1)$$

III. VARIABLE STIFFNESS MONO- AND BI-ARTICULAR ACTUATOR STRUCTURES

A. Structure

In Fig. 2 two actuation structures for a two-link intrinsically compliant robot arm actuated by VSAs are shown. The structure shown in Fig. 2(a) will be referred to as Variable

Stiffness Monoarticular Actuator (VSMA). VSMA is the conventional structure implemented in intrinsically compliant robot arms. It consists of two VSAs, each connected to one joint as monoarticular actuators. Each VSA is made of two motors in an antagonistic configuration and two nonlinear springs. The structure shown in Fig. 2(b) will be referred to as Variable Stiffness Biarticular Actuator (VSBA). The VSBA structure consists of one VSA connected to joint 1 as a monoarticular actuator, and a VSA connected to both joints 1 and 2 as a biarticular actuator by mean of a free pulley system.

B. Modeling

Given the reference system in Fig. 2(a), the spring displacements between joints and respective actuator for the VSMA structure are:

$$\Delta l_{\phi 1} = \phi_1 r_m - r_1 \theta_1 \tag{2}$$
$$\Delta l_{\varepsilon 1} = \varepsilon_1 r_m + r_1 \theta_1 \tag{3}$$
$$\Delta l_{\phi 2} = \phi_2 r_m - r_2 \theta_2 \tag{4}$$
$$\Delta l_{\varepsilon 2} = \varepsilon_2 r_m + r_2 \theta_2 \tag{5}$$

where ϕi and εi are respectively the flexor and extensor monoarticular actuator angle displacements in radians, $\boldsymbol{\theta} = [\theta_1, \theta_2]^{\mathrm{T}}$ is the joint angle position in radians, r_m is the radius of the motor pulleys, and r_1 and r_2 are the radii of pulleys at joint 1 and 2, respectively.

The force-displacement characteristic of the springs is of quadratic form, therefore the resulting forces $f_{(\phi i, \varepsilon i)}$ are:

$$f_{\phi 1} = k_2 \Delta l_{\phi 1}^2 + k_1 \Delta l_{\phi 1} + k_0 \tag{6}$$
$$f_{\varepsilon 1} = k_2 \Delta l_{\varepsilon 1}^2 + k_1 \Delta l_{\varepsilon 1} + k_0 \tag{7}$$
$$f_{\phi 2} = k_2 \Delta l_{\phi 2}^2 + k_1 \Delta l_{\phi 2} + k_0 \tag{8}$$
$$f_{\varepsilon 2} = k_2 \Delta l_{\varepsilon 2}^2 + k_1 \Delta l_{\varepsilon 2} + k_0 \tag{9}$$

where k_0, k_1, k_2 are the quadratic spring constants.

The joint torques ($\boldsymbol{T}^{VSMA}$) are:

$$\begin{aligned} \boldsymbol{T}^{VSMA} &= \begin{bmatrix} T_1^{VSMA} \\ T_2^{VSMA} \end{bmatrix} = \begin{bmatrix} \tau_1 \\ \tau_2 \end{bmatrix} = \begin{bmatrix} r_1(f_{\phi 1} - f_{\varepsilon 1}) \\ r_2(f_{\phi 2} - f_{\varepsilon 2}) \end{bmatrix} \\ &= \begin{bmatrix} k_2 r_1(\Delta l_{\phi 1}^2 - \Delta l_{\varepsilon 1}^2) + k_1 r_1(\Delta l_{\phi 1} - \Delta l_{\varepsilon 1}) \\ k_2 r_2(\Delta l_{\phi 2}^2 - \Delta l_{\varepsilon 2}^2) + k_1 r_2(\Delta l_{\phi 2} - \Delta l_{\varepsilon 2}) \end{bmatrix} \end{aligned} \tag{10}$$

where τ_i is the torque resulting at joint i produced by the monoarticular actuator i.

The joint stiffness matrix is:

$$\boldsymbol{Kj}^{VSMA} = \left(\boldsymbol{Jt}^{VSMA}\right)^T \boldsymbol{Kt}^{VSMA} \boldsymbol{Jt}^{VSMA} \tag{11}$$

$$= \begin{bmatrix} 2r_1^2(k_2(\Delta l_{\phi 1} + \Delta l_{\varepsilon 1}) + k_1) & 0 \\ 0 & 2r_2^2(k_2(\Delta l_{\phi 2} + \Delta l_{\varepsilon 2}) + k_1) \end{bmatrix} \tag{12}$$

where

$$\left(\boldsymbol{Jt}^{VSMA}\right)^T = \begin{bmatrix} r_1 & -r_1 & 0 & 0 \\ 0 & 0 & r_2 & -r_2 \end{bmatrix} \tag{13}$$

$$\boldsymbol{Kt}^{VSMA} = \begin{bmatrix} 2k_2\Delta l_{\phi 1} + k_1 & 0 & 0 & 0 \\ 0 & 2k_2\Delta l_{\varepsilon 1} + k_1 & 0 & 0 \\ 0 & 0 & 2k_2\Delta l_{\phi 2} + k_1 & 0 \\ 0 & 0 & 0 & 2k_2\Delta l_{\varepsilon 2} + k_1 \end{bmatrix} \tag{14}$$

For the VSBA structure, given the reference system in Fig. 2(b), the spring displacements between joints and respective actuator are:

$$\Delta l_{\phi 1} = \phi_1 r_m - r_1 \theta_1 \tag{15}$$
$$\Delta l_{\varepsilon 1} = \varepsilon_1 r_m + r_1 \theta_1 \tag{16}$$
$$\Delta l_{\phi 12} = \phi_{12} r_m - r_{12} \theta_1 - r_2 \theta_2 \tag{17}$$
$$\Delta l_{\varepsilon 12} = \varepsilon_{12} r_m + r_{12} \theta_1 + r_2 \theta_2 \tag{18}$$

where ϕ_{12} and ε_{12} are respectively the flexor and extensor biarticular actuator angle displacements in radians, r_{12} is the radius of the free pulley about joint 1 through which the biarticular actuators produce torque about joint 1.

The forces produced by the springs are:

$$f_{\phi 1} = k_2 \Delta l_{\phi 1}^2 + k_1 \Delta l_{\phi 1} + k_0 \tag{19}$$
$$f_{\varepsilon 1} = k_2 \Delta l_{\varepsilon 1}^2 + k_1 \Delta l_{\varepsilon 1} + k_0 \tag{20}$$
$$f_{\phi 12} = k_2 \Delta l_{\phi 12}^2 + k_1 \Delta l_{\phi 12} + k_0 \tag{21}$$
$$f_{\varepsilon 12} = k_2 \Delta l_{\varepsilon 12}^2 + k_1 \Delta l_{\varepsilon 12} + k_0 \tag{22}$$

The joint torque ($\boldsymbol{T}^{VSBA}$) are:

$$\begin{aligned} \boldsymbol{T}^{VSBA} &= \begin{bmatrix} T_1^{VSBA} \\ T_2^{VSBA} \end{bmatrix} = \begin{bmatrix} \tau_1 + \tau_3 \\ \tau_3 \end{bmatrix} \\ &= \begin{bmatrix} r_1(f_{\phi 1} - f_{\varepsilon 1}) + r_{12}(f_{\phi 12} - f_{\varepsilon 12}) \\ r_2(f_{\phi 12} - f_{\varepsilon 12}) \end{bmatrix} \end{aligned} \tag{23}$$

where τ_1 is the torque resulting at joint 1 produced by the monoarticular actuators ϕ_1 and ε_1, τ_3 is the torque resulting at joints 1 and 2 produced by the biarticular actuators ϕ_{12} and ε_{12}, respectively.

By combining (19)–(23) the joint torques are expressed by:

$$\begin{aligned} T_1^{VSBA} = {} & k_2 r_{12}(\Delta l_{\phi 12}^2 - \Delta l_{\varepsilon 12}^2) + k_1 r_{12}(\Delta l_{\phi 12} - \Delta l_{\varepsilon 12}) \\ & + k_2 r_1(\Delta l_{\phi 1}^2 - \Delta l_{\varepsilon 1}^2) + k_1 r_1(\Delta l_{\phi 1} - \Delta l_{\varepsilon 1}) \end{aligned} \tag{24}$$

$$T_2^{VSBA} = k_2 r_2(\Delta l_{\phi 12}^2 - \Delta l_{\varepsilon 12}^2) + k_1 r_2(\Delta l_{\phi 12} - \Delta l_{\varepsilon 12}) \tag{25}$$

The joint stiffness matrix is:

$$\begin{aligned} \boldsymbol{Kj}^{VSBA} &= \left(\boldsymbol{Jt}^{VSBA}\right)^T \boldsymbol{Kt}^{VSBA} \boldsymbol{Jt}^{VSBA} \\ &= \begin{bmatrix} Kj_{11}^{VSBA} & Kj_{12}^{VSBA} \\ Kj_{21}^{VSBA} & Kj_{22}^{VSBA} \end{bmatrix} \end{aligned} \tag{26}$$

where,

$$\left(\boldsymbol{Jt}^{VSBA}\right)^T = \begin{bmatrix} r_1 & -r_1 & r_{12} & -r_{12} \\ 0 & 0 & r_2 & -r_2 \end{bmatrix} \tag{27}$$

TABLE I

PARAMETERS VALUES

$L_1 = L_2$	1 (m)
Pulleys radii $r_m = r_1 = r_2 = r_{12}$	0.1 (m)
k_0, k_1	$2, -200$ (N/m)
k_2	10^5 (N^2/m^2)
All motors maximum torque ($\tau_{\text{motor}}^{\max}$)	10 (Nm)
Minimum co-contraction force	5 (N)

$$\boldsymbol{Kt}^{\boldsymbol{VSBA}} = \begin{bmatrix} 2k_2\Delta l_{\phi 1} + k_1 & 0 \\ 0 & 2k_2\Delta l_{\varepsilon 1} + k_1 \\ 0 & 0 \\ 0 & 0 \\ 0 & 0 \\ 0 & 0 \\ 2k_2\Delta l_{\phi 12} + k_1 & 0 \\ 0 & 2k_2\Delta l_{\varepsilon 12} + k_1 \end{bmatrix} \tag{28}$$

$$\begin{aligned} Kj_{11}^{VSBA} =& 2r_{12}^2(k_2\Delta l_{\phi 12} + k_2\Delta l_{\varepsilon 12} + k_1) \\ &+ 2r_1^2(k_2\Delta l_{\phi 1} + k_2\Delta l_{\varepsilon 1} + k_1) \end{aligned} \tag{29}$$

$$Kj_{12}^{VSBA} = Kj_{21}^{VSBA} = 2r_{12}r_2(k_2\Delta l_{\phi 12} + k_2\Delta l_{\varepsilon 12} + k_1) \tag{30}$$

$$Kj_{22}^{VSBA} = r_2^2(k_2\Delta l_{\phi 12} + k_2\Delta l_{\varepsilon 12} + k_1) \tag{31}$$

From (26) emerges the role of biarticular actuator in stiffness modulation. Biarticular actuation can modulate the stiffness in both joints at the same time.

The stiffness matrix in Cartesian coordinates of the two actuation structures, $\boldsymbol{K}^{(VSMA,VSBA)}$, is:

$$\boldsymbol{K}^{(VSMA,VSBA)} = \left(\boldsymbol{J}^{\mathrm{T}}\right)^{-1} \boldsymbol{Kj}^{(VSMA,VSBA)} (\boldsymbol{J})^{-1} \tag{32}$$

where $\boldsymbol{J}$ is the robot arm analytical Jacobian matrix:

$$\boldsymbol{J} = \begin{bmatrix} -L_1\sin(\theta_1) - L_2\sin(\theta_1+\theta_2) & -L_2\sin(\theta_1+\theta_2) \\ L_1\cos(\theta_1) + L_2\cos(\theta_1+\theta_2) & L_2\cos(\theta_1+\theta_2) \end{bmatrix} \tag{33}$$

The parameters of the two-link arm and the two actuation structures used in this work are shown in Tab. I. The parameters for the quadratic springs have been chosen as an approximation of the values of the quadratic springs used in [5]. Every pulley radii, as well every maximum motor torque, have been chosen with same value, therefore all the maximum joint actuator torques is same.

IV. ANALYSIS METHOD

The VSMA and the VSBA structures are compared in terms of end effector stiffness isotropy. Three robot arm configurations are considered: $\boldsymbol{\theta} = [0, 30^\circ]^T$ (stretched arm), $\boldsymbol{\theta} = [0, 90^\circ]^T$ (in a central zone of the workspace), $\boldsymbol{\theta} = [0, 150^\circ]^T$ (bended arm). The end effector stiffness isotropy is compared using the condition number (cn) of minimum and maximum Cartesian stiffness defined as [30]:

$$cn_{(minsti,maxsti)}^{(VSMA,VSBA)} = \frac{\max(\lambda(\boldsymbol{K}_{(minsti,maxsti)}^{(VSMA,VSBA)}))}{\min(\lambda(\boldsymbol{K}_{(minsti,maxsti)}^{(VSMA,VSBA)}))} \tag{34}$$

TABLE II

END EFFECTOR CARTESIAN STIFFNESS MATRICES

	$\boldsymbol{\theta}$		
	$\boldsymbol{\theta} = [0, 30^\circ]^T$	$\boldsymbol{\theta} = [0, 90^\circ]^T$	$\boldsymbol{\theta} = [0, 150^\circ]^T$
$\boldsymbol{K}_{minsti}^{VSMA}$	$\begin{bmatrix} 135.4 & 43.7 \\ 43.7 & 16 \end{bmatrix}$	$\begin{bmatrix} 8 & 8 \\ 8 & 16 \end{bmatrix}$	$\begin{bmatrix} 24.6 & -11.7 \\ -11.7 & 16 \end{bmatrix}$
cn_{minsti}^{VSMA}	87.6	6.86	4.1
$\boldsymbol{K}_{maxstii}^{VSMA}$	$\begin{bmatrix} 637.7 & 217.5 \\ 217.5 & 79.6 \end{bmatrix}$	$\begin{bmatrix} 39.8 & 39.8 \\ 39.8 & 79.6 \end{bmatrix}$	$\begin{bmatrix} 122.3 & -58.3 \\ -58.3 & 79.6 \end{bmatrix}$
cn_{maxsti}^{VSMA}	87.6	6.86	4.1
$\boldsymbol{K}_{minsti}^{VSBA}$	$\begin{bmatrix} 56 & 13.9 \\ 13.9 & 8 \end{bmatrix}$	$\begin{bmatrix} 8 & 0 \\ 0 & 8 \end{bmatrix}$	$\begin{bmatrix} 56 & -13.9 \\ -13.9 & 8 \end{bmatrix}$
cn_{minsti}^{VSBA}	13.9	1	13.9
$\boldsymbol{K}_{maxstii}^{VSBA}$	$\begin{bmatrix} 278.6 & 68.9 \\ 68.9 & 39.8 \end{bmatrix}$	$\begin{bmatrix} 4 & 0 \\ 0 & 4 \end{bmatrix}$	$\begin{bmatrix} 278.6 & -68.9 \\ -68.9 & 39.8 \end{bmatrix}$
cn_{maxsti}^{VSBA}	13.9	1	13.9

where $\lambda(\boldsymbol{K})$ are the eigenvalues of the stiffness matrix in Cartesian coordinates ($\boldsymbol{K}^{(VSMA,VSBA)}$ in (32)).

The condition number ($cn \in [1, \infty)$) expresses the isotropy of the Cartesian stiffness ellipse at the end effector. The minimum value of the condition number is 1, representing the highest isotropic condition (i.e the circle). The higher the condition number, the lower the isotropy of the ellipse. The minimum (or maximum) Cartesian stiffness (indicated with the suffix minsti and maxsti in (34) is calculated when the end effector force is null and the antagonistic actuators co-contraction force is minimum (5 N) or maximum (100 N).

V. RESULTS

In Tab. II the minimum and maximum Cartesian stiffness matrices calculated using (32) for both actuation structures are shown for three arm configurations: $\boldsymbol{\theta} = [0, 30^\circ]^T$, $\boldsymbol{\theta} = [0, 90^\circ]^T$, $\boldsymbol{\theta} = [0, 150^\circ]^T$.

In addition, the resulting condition numbers calculated using (34) are shown. Due to the symmetry in agonistic-antagonistic actuation in both the structures — VSMA and VSBA — the condition numbers of maximum and minimum stiffnesses are identical. It is noticeable that, for the configuration in which $\boldsymbol{\theta} = [0, 90^\circ]^T$, the condition number for the VSBA structure is 1, meaning that a stiffness has the same value in any direction. The same happens for the VSMA structure when $\boldsymbol{\theta} = [0, 180^\circ]^T$ (a singular configuration). A graphical representation of the minimum and maximum Cartesian stiffnesses of Tab. II is shown in Fig. 3. The stiffness magnitude is plotted in respect to its direction in the reference frame of Fig. 1(b)

In order to compare the stiffness isotropy, the condition numbers of Cartesian stiffness for both actuation structure is shown in Fig. 4. The VSBA structure presents a lower end effector isotropy when $\theta_2 > 120^\circ$, while a higher isotropy when $\theta_2 < 120^\circ$.

Based on the results of Fig. 4, in Fig. 5 the regions of the workspace of the two-link robot arm where the VSMA and VSBA are advantageous in terms of stiffness isotropy are shown.

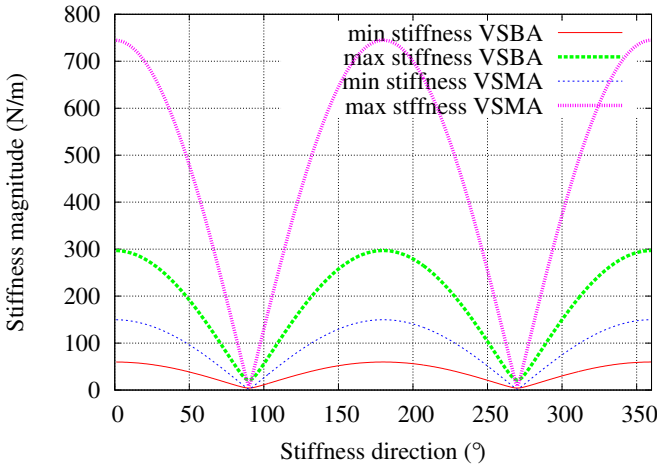

(a) $\boldsymbol{\theta} = [0, 30°]^T$

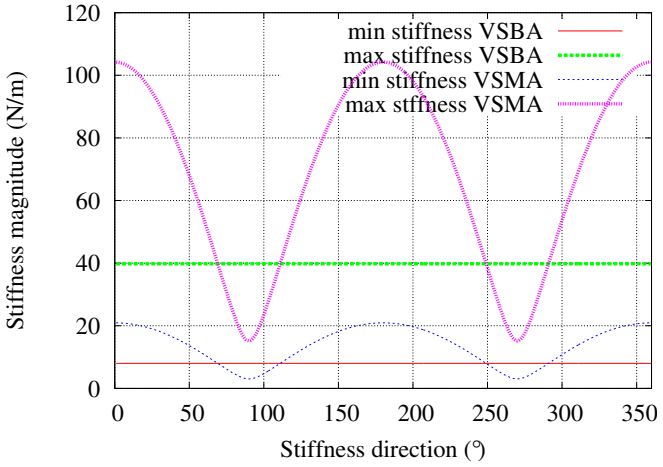

(b) $\boldsymbol{\theta} = [0, 90°]^T$

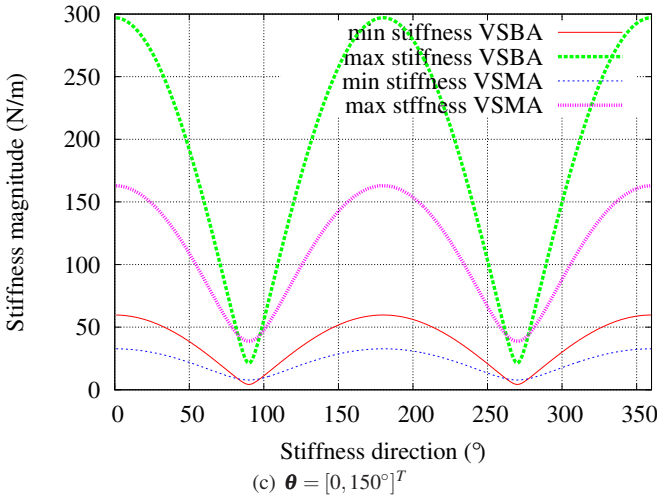

(c) $\boldsymbol{\theta} = [0, 150°]^T$

Fig. 3. Minimum and maximum end effector Cartesian stiffness

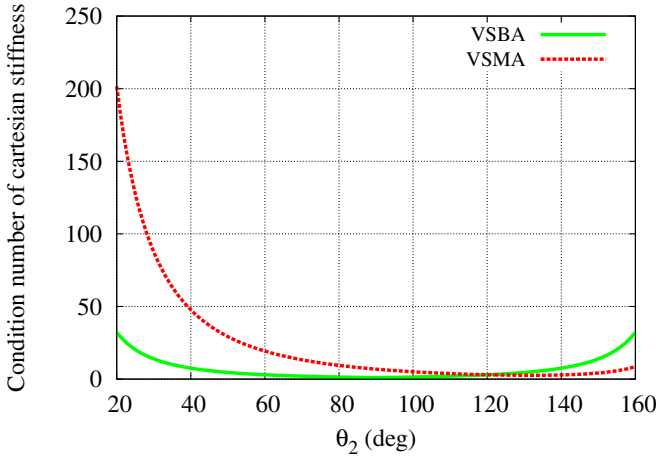

Fig. 4. Condition numbers of Cartesian stiffness in respect to θ_2

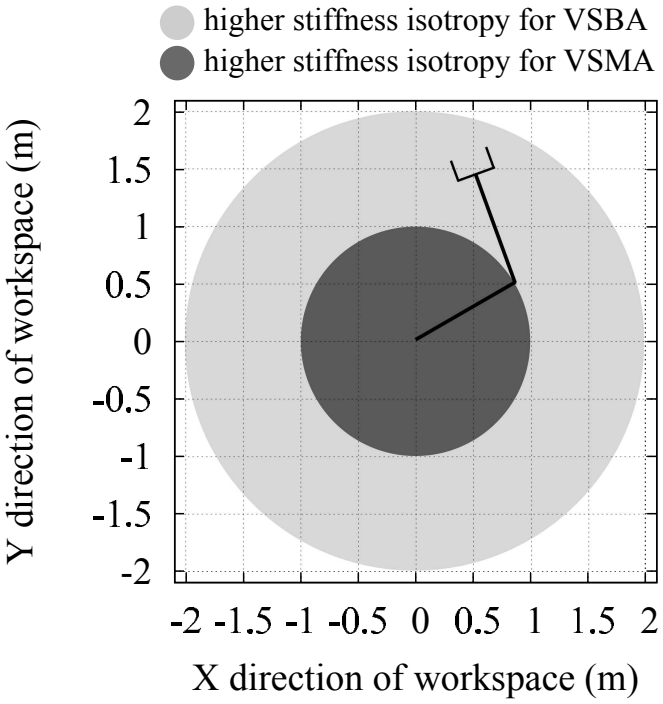

Fig. 5. Regions of the workspace of the two-link robot arm where the VSMA and VSBA are advantageous in terms of stiffness isotropy

The VSBA structure is advantageous in the outer region of the workspace in terms of stiffness isotropy. It is in this region that manipulators typically execute dynamic tasks requiring stiffness modulation: for example opening/closing doors for robot arms, or walking, running, and jumping for legged robots. In addition, a stretched configuration of the manipulator (operating in the outer region of the workspace) is more challenging to control due to the increasing non-linearities of the Jacobian matrix. A higher isotropy in such condition is therefore favorable to have homogeneous response to disturbances.

VI. CONCLUSIONS

End effector stiffness isotropy is a key aspect for safety and performance of intrinsically compliant manipulators. In

this work, we evaluate the end effector intrinsic stiffness isotropy of a two-link planar arm with Variable Stiffness Actuators (VSAs). Two actuation structures — the traditional monoarticular and human-like biarticular — are taken into account.

Results show that the human-like biarticular structure is advantageous from a stiffness isotropy point of view in the outer (radial) half of the workspace. This region is where manipulators most frequently execute dynamic tasks requiring passive stiffness modulation, and is more challenging in control due to increased geometrical nonlinearities (i.e. the Jacobian matrix). Therefore, human-like biarticular structure better suits the requirements of intrinsically compliant manipulators, such as robotic arms (for example when opening or closing doors) or legs (walking, running, jumping).

Future works include the experimental validation of the analytical analysis carried out in this work.

ACKNOWLEDGMENT

This work is supported by Japan Society for Promotion of Science (JSPS), JSPS KAKENHI Grant Number 24.02748.

REFERENCES

[1] A. Bicchi, S. Rizzini, and G. Tonietti, "Compliant design for intrinsic safety: general issues and preliminary design," in *2001 IEEE/RSJ International Conference on Intelligent Robots and Systems, 2001. Proceedings*, vol. 4, 2001, pp. 1864–1869 vol.4.

[2] G. A. Pratt and M. M. Williamson, "Series elastic actuators," in *Intelligent Robots and Systems 95.'Human Robot Interaction and Cooperative Robots', Proceedings. 1995 IEEE/RSJ International Conference on*, vol. 1, 1995, pp. 399–406.

[3] C. English and D. Russell, "Mechanics and stiffness limitations of a variable stiffness actuator for use in prosthetic limbs," *Mechanism and Machine Theory*, vol. 34, no. 1, pp. 7–25, Jan. 1999.

[4] R. Ham, T. Sugar, B. Vanderborght, K. Hollander, and D. Lefeber, "Compliant actuator designs," *IEEE Robotics Automation Magazine*, vol. 16, no. 3, pp. 81–94, 2009.

[5] S. Migliore, E. Brown, and S. DeWeerth, "Biologically inspired joint stiffness control," in *International Conference on Robotics and Automation (ICRA)*, 2005, pp. 4508–4513.

[6] J. Hurst, J. Chestnutt, and A. Rizzi, "The actuator with mechanically adjustable series compliance," *IEEE Transactions on Robotics*, vol. 26, no. 4, pp. 597–606, 2010.

[7] N. G. Tsagarakis, M. Laffranchi, B. Vanderborght, and D. Caldwell, "A compact soft actuator unit for small scale human friendly robots," in *International Conference on Robotics and Automation (ICRA)*, 2009, pp. 4356–4362.

[8] G. Palli, C. Melchiorri, T. Wimbock, M. Grebenstein, and G. Hirzinger, "Feedback linearization and simultaneous stiffness-position control of robots with antagonistic actuated joints," in *International Conference on Robotics and Automation (ICRA)*, 2007, pp. 4367–4372.

[9] M. A. Daley, J. R. Usherwood, G. Felix, and A. A. Biewener, "Running over rough terrain: guinea fowl maintain dynamic stability despite a large unexpected change in substrate height," *J Exp Biol*, vol. 209, no. 1, pp. 171–187, Jan. 2006.

[10] J. B. Smeets, "Bi-articular muscles and the accuracy of motor control," *Human Movement Science*, vol. 13, no. 5, pp. 587–600, Oct. 1994.

[11] G. J. Van Ingen Schenau, "From rotation to translation: Constraints on multi-joint movements and the unique action of bi-articular muscles," *Human Movement Science*, vol. 8, no. 4, pp. 301–337, Aug. 1989.

[12] R. Jacobs and G. J. van Ingen Schenau, "Control of an external force in leg extensions in humans." *The Journal of Physiology*, vol. 457, no. 1, pp. 611 –626, Nov. 1992.

[13] N. Hogan, "Impedance control: An approach to manipulation: Part III—Applications," *Journal of Dynamic Systems, Measurement, and Control*, vol. 107, no. 1, pp. 17–24, Mar. 1985.

[14] V. Salvucci, S. Oh, Y. Hori, and Y. Kimura, "Disturbance rejection improvement in non-redundant robot arms using bi-articular actuators," in *Intern. Symp. on Industrial Electronics (ISIE)*, 2011, pp. 2159–2164.

[15] V. Salvucci, Y. Kimura, S. Oh, and Y. Hori, "Non-linear phase different control for precise output force of bi-articularly actuated manipulators," *Advanced Robotics*, vol. 27, no. 2, pp. 109–120, 2013.

[16] S. Oh, Y. Kimura, and Y. Hori, "Reaction force control of robot manipulator based on biarticular muscle viscoelasticity control," in *Advanced Intelligent Mechatronics (AIM)*, 2010, pp. 1105–1110.

[17] V. Salvucci, Y. Kimura, S. Oh, T. Koseki, and Y. Hori, "Comparing approaches for actuator redundancy resolution in bi-articularly actuated robot arms," *Mechatronics, IEEE/ASME Transactions on*, May 2013.

[18] K. Hosoda, Y. Sakaguchi, H. Takayama, and T. Takuma, "Pneumatic-driven jumping robot with anthropomorphic muscular skeleton structure," *Autonomous Robots*, vol. 28, no. 3, pp. 307–316, Dec. 2009.

[19] Y. Nakata, A. Ide, Y. Nakamura, K. Hirata, and H. Ishiguro, "Hopping of a monopedal robot with a biarticular muscle driven by electromagnetic linear actuators," in *2012 IEEE International Conference on Robotics and Automation (ICRA)*, May 2012, pp. 3153 –3160.

[20] T. Tsuji, "A model of antagonistic triarticular muscle mechanism for lancelet robot," in *2010 11th IEEE International Workshop on Advanced Motion Control*. IEEE, Mar. 2010, pp. 496–501.

[21] Y. Kimura, S. Oh, and Y. Hori, "Novel robot arm with bi-articular driving system using a planetary gear system and disturbance observer," in *International Workshop on Advanced Motion Control (AIM)*, 2010, pp. 296–301.

[22] V. Salvucci, Y. Kimura, S. Oh, and Y. Hori, "BiWi: bi-articularly actuated and wire driven robot arm," in *IEEE International Conference on Mechatronics (ICM)*, Apr. 2011, pp. 827–832.

[23] M. A. Lewis and T. J. Klein, "Achilles: A robot with realistic legs," in *IEEE Biomedical Circuits and Systems Conference (BIOCAS)*, 2008.

[24] A. Seyfarth, F. Iida, R. Tausch, M. Stelzer, O. von Stryk, and A. Karguth, "Towards bipedal jogging as a natural result of optimizing walking speed for passively compliant Three-Segmented legs," *Intern. Journal of Robotics Research*, vol. 28, no. 2, pp. 257 –265, 2009.

[25] M. Chalon, T. Wimbock, and G. Hirzinger, "Torque and workspace analysis for flexible tendon driven mechanisms," in *International Conference on Robotics and Automation (ICRA)*, 2010, pp. 1175–1181.

[26] H. Fukusho, T. Sugimoto, and T. Koseki, "Control of a straight line motion for a two-link robot arm using coordinate transform of bi-articular simultaneous drive," in *Advanced Motion Control, 2010 11th IEEE International Workshop on*, 2010, pp. 786–791.

[27] M. Kumamoto, T. Oshima, and T. Yamamoto, "Control properties induced by the existence of antagonistic pairs of bi-articular muscles – mechanical engineering model analyses," *Human Movement Science*, vol. 13, no. 5, pp. 611–634, Oct. 1994.

[28] S. Oh, V. Salvucci, and Y. Hori, "Development of simplified statics of robot manipulator and optimized muscle torque distribution based on the statics," in *American Control Conference (ACC)*, Jul. 2011, pp. 4099–4104.

[29] V. Salvucci, Y. Kimura, S. Oh, and Y. Hori, "Experimental verification of infinity norm approach for force maximization of manipulators driven by bi-articular actuators," in *American Control Conference (ACC)*, 2011.

[30] N. Kashiri, N. G. Tsagarakis, M. Laffranchi, and D. G. Caldwell, "On the stiffness design of intrinsic compliant manipulators," in *2013 IEEE/ASME International Conference on Advanced Intelligent Mechatronics (AIM)*, 2013, pp. 1306–1311, 00000.